Novelty Journals

ISSN 2394-7314

International Journal of Novel Research in Computer Science and Software Engineering
Vol. 11, Issue 2, pp: (25-44), Month: May - August 2024, Available at: www.noveltyjournals.com

A Deep Learning Hybridized Model for Segmentation of Medical Brain Tumors

Gani Timothy Abe[1], Philemon Uten Emmoh[2,]

Department of Computer Science, Federal University Wukari, Taraba State, Nigeria[1,2].

DOI: https://doi.org/10.5281/zenodo.11574304

Published Date: 11-June-2024

Abstract: **This study conducted a comprehensive analysis of online brain tumor scan data, developing and evaluating a robust model to discern Intracranial Neoplasm brain tumors. Employing an empirical approach, we utilized Mask-RCNN and U-net for segmenting Intracranial Neoplasm tumors from brain Magnetic Resonance Images (MRIs). Our methodology encompassed dataset elucidation, data pre-processing, network architecture, training, testing strategies, and proposed ensemble methods. The dataset comprising 253 brain tumors and employed U-nets and Mask-RCNN, utilizing a statistical confusion matrix to evaluate tumor stratification performance, differentiating true positives (Tp), true negatives (Tn), false positives (Fp), and false negatives (Fn). Employing deep learning techniques and Python programming, using Accuracy, Sensitivity, Specificity, Dice coefficient, and Jaccard index metrics. Our findings revealed that the 176-training brain tumor dataset samples, 95 identified as "yes" tumors, while 5 misclassified as "no" tumors. For the testing set comprising 77 cases, 42 "yes" tumors were identified, along with 26 "no" tumors. The training model achieved remarkable performance metrics, boasting 93% accuracy, 95% sensitivity, and 90% specificity, with a 96% similarity to ground truth. The testing set results showcased 89% sensitivity, 86% Specificity, and 88% accuracy, across 253 cases, our model demonstrated 92% sensitivity, 88% specificity, and 90.5% accuracy. The model's runtime for segmenting the 176 datasets was 466 seconds, approximately 7 minutes and 45 seconds. In conclusion, our study yields highly satisfactory results with an accuracy of 90.5%, 92% sensitivity, and 88% specificity. This model exhibits promising potential for precise brain tumor boundary detection, enhancing segmentation, diagnosis, and guiding brain tumor surgery.**

Keywords: **Machine Learning; Convolutional Neural Network; U-nets, Mask-RCNN; Segmentation; Magnetic Resonance Images; and Brain Tumor.**

1. INTRODUCTION

Deep Learning is a branch of machine learning that has gained popularity in recent years for creating automatic, semi-automatic, or hybrid models that can effectively identify and segment tumors with the highest level of accuracy in the shortest amount of time (Bhatele & Bhadauria, 2020). When dealing with brain tumor issues, at the moment, the most widely used methods for analyzing brain tumor images are DL-based approaches. Whereby the most widely used Deep Learning models for brain tumor identification, segmentation, and classification are the convolutional neural networks (CNN), recurrent neural networks (RNN), visual geometry groups (VGG), ResNet, Inception, autoencoders, U-Nets, and their variants (Nazir et al., 2021). With the introduction of artificial intelligence research and the warm-up of in-depth learning research in image processing, convolution neural network (CNN) has gained a lot of interest (LeCun et al., 1999). It is very accurate for image classification because of its great efficiency for feature extraction and the particular classification model developed through learning (Chen *et al.*, 2016). CNN has a lot of success with image classification (He et al., 2016; Krizhevsky et al., 2012), segmentation and detection (Sermanet et al., 2013; Long et al., 2015; Chen et al., 2014; Long et al., 2015). CNN retains a low computational complexity as compared to manual image pre-processing,

filtering, and convolution. Convolutional network is among the most well-known neural networks that are commonly utilized in image identification. However, despite the fact that such methodology has shown to be effective, tumors remain difficult to segment in large medical images, particularly the brain. Computational costs from thousands of operations on input images such as convolutions, pooling, and oversampling of the CNN architecture are extremely expensive (Mlynarski et al., 2019). In this context, tasks involving segmentation in sizeable pathological image such as CT or MRI scans are extremely challenging to execute. Despite the advancement of new neural network topologies, 3-dimensional image modelling remains a difficult task for CNN-based systems. Theoretically, these methods on the one hand could use different modalities of MR images to segment specific parts of organs or tissues in patients and the corrected automation of this segmentation (Mlynarski et al., 2019). On the other hand, in practice, the conditions are insufficient for implementation. Benign and malignant brain tumors are considered as the two basic types of brain tumors. Benign tumors are generally uncommon, grow slowly, and do not spread. On the other hand, malignant brain tumors are made up of cancerous cells and typically begin in one part of the brain rapidly spread to other parts of the brain and spinal cord (Ayadi et al., 2021). Based on how they behave within the brain, the World Health Organization (WHO) defines brain tumors into four distinct groups: which grades 1 and grade 2 are regarded as low-grade or benign tumors, while grades 3 and 4 are classified as high-grade or malignant tumors. Magnetic resonance imaging (MRI) is the most dependable and often used diagnostic technique for brain tumor detection. Other diagnostic techniques include CT scanning and electroencephalography (EEG). MRI uses radio waves and strong magnetic fields to provide detailed interior images of the body's organs (Badža & Barjaktarović, 2020). Also, the magnetic resonance imaging (MRI) scans, which are non-invasive and offer high-resolution and comprehensive information on soft tissues, are typically used to analyze the structure of the brain. The regions that appear distinct from normal tissues in the brain tumors can be identified through segmentation process. Gliomas are inherently more difficult to segment than meningiomas, although certain tumors, like meningiomas, can easily be isolated. It is challenging to perform the division process since these brain tumors are frequently disseminated, exhibit edema, and have features that resemble extended limbs. Often, it is difficult to discern their boundaries from those of healthy tissues since they are so fuzzy. likewise, they can manifest in any part of the brain and come in a variety of sizes and forms (Soltaninejad et al., 2017) .

This research focuses on model-based image segmentation tasks in medical applications for brain tumors using deep learning techniques. The goal is to implement a suitable deep learning algorithm to exhibit or present its usefulness in segmenting 2D-3D medical images of a brain tumor.

The study outlining its purpose, problem statement, research objectives, justification, and thesis organization. The subsequent chapters are structured as follows: Section 2 focuses on a literature review of biomedical image segmentation, covering theoretical background, datasets, segmentation methods, machine learning applications, and model evaluation. Section 3 details the methodology, emphasizing the use of Mask R-CNN and U-net for segmenting brain tumors from MRI scans. It covers data collection, pre-processing, network design, training, testing, and conceptual perspectives on CNN architecture. Section 4 presents experimental results and discusses them in relation to prior findings. Section 5 continues the discussion of results and their implications. Section 6 provides recommendations, conclusions, discusses knowledge contributions, and suggests future research directions.

2. LITERATURE REVIEW

Researchers have developed many approaches to automatic segmentation (Withey and Koles, 2007). However, fully automatic segmentation approach rarely yields precise and reliable findings that are clinically important (Sharma and Aggarwal, 2010). Poor image quality, noise, partial volume effect, artifacts, and low contrast differ across individual patients. Disease-induced non-homogeneous appearances and physician variability in procedures contribute to differing precision of structural boundaries. Despite extensive researches and promising advancements in medical image processing, computerized 2D and the 3D, brain tumor segmentation remains a difficult task. CNNs (Milletari *et al.*, 2016; Bakator and Radosav, 2018), U-Net, Mask – RCNN (He *et al.*, 2017) and De-convolutional network (Işn *et al.*, 2016) in recent research have all been widely used (Noh *et al.*, 2015). In the past, within the BraTS dataset, challenges and additional issues related to semantic and biomedical segmentation were encountered. CNN has demonstrated its usefulness and has over time recorded success in automatically classifying normal and diseased in brain MRI data. Reviews of individual articles in deep learning and medical diagnosis are hereby discussed.

Cernazanu-Glavan and Holban (2013) proposed a technique for segmenting X-ray image that uses a CNN as a pixel classifier. The algorithm scrutinized every single pixel in the image and categorizes them into two groups: bone or non-bone. Using segmentation process, it attempted to segment the bone from tissues for the rest of the image. CNN emerged the best when compared to alternative setups. They used the image's areas of interest to achieve a short network training period. Their approach detected substantial bone regions. However, issues arose when the bone area displayed abnormalities and required longer time to train.

Bandhyopadhyay and Paul (2013) proposed a K-means clustering-based brain tumor segmentation approach. There are three phases to the method: (i) Segmentation using K-means approach, (ii) grid-based scratchy grist localization of function guide by standard deviation and (iii) grid-based feathery grist localization of function guide by standard deviation. The research used over a hundred MRI images which recorded success in more than 97% tumor identification cases. Abdel-Maksoud *et al.* (2015) proposed segmentation of brain tumor by using a hybridized clustering method. They combine the K-means clustering approach with the Fuzzy C-means algorithm for reliable and fast diagnosis of the brain tumors. The model was validated by (i) pre-processing; de-noising and skull removal, (ii). Clustering; K-means and Fuzzy C-means integration, (iii) extraction and (iv) contouring; thresholding and level set are the validation processes. Comparing these brain tumor segmentation approaches against four cutting-edge algorithms, such as Fuzzy C-means, Mean-shift, K-means and the Expectation-Maximization, the researcher was competent to establish its effectiveness.

Nabizadeh and Kubat (2015) developed a fully automated method for identifying and segmenting brain cancers using magnetic resonance imaging. To detect slices containing tumors and outline the tumor region, they employed Gabor wavelet vs. statistical characteristics. The classification accuracies of k-means using Euclidean and city-block distances are 83.2 ± 0.1% and 85.4 ± 0.1% for statistical features, and 69.6 ± 0.3% and 71.3 ± 0.2% for Gabor wavelet features, respectively.

Zhao *et al.* (2016) developed a novel approached for segmentation of brain tumor that incorporates both Fully Convolutional Neural Network (FCNN) and Conditional Random Fields (CRF). They trained this model in three phases by using group of pixels in image and slices. Each MR image was pre-processed with N4ITK and intensity normalization. Some 3D-connected areas were eliminated and labels of chosen pixels were adjusted with simple thresholding method so as to post-process the segmentation results. On the same BRATS 2013 dataset, the findings demonstrated that these tactics were successful when compared to other methodologies.

Pereira *et al.* (2016) developed CNN-based automated segmentation approach that explored small 3 x 3 kernels. The proposed model was evaluated using brain tumor challenge BRATS dataset (2013). The data were calculated in two different phases using the Dice Similarity Coefficient metric. In the calculation, there is total, core, and enhancing regions, and they all received the highest Dice scores. Total: 0.88%; core: 0.83% and enhancing: 0.77%; whereas, the total, core, and enhancing areas received the lowest Dice scores; Total: 0.78%; core 0.65% and enhancing: 0.75%.

Amin *et al.* (2017) presented and suggested a novel MRI-based brain tumor detection and classification method. They applied an SVM classifier and validated the model on three datasets such as RIDER, Harvard, and Local. The result came out with the average achievement of 0.98 areas under curve, an accuracy of 97.1%, 91.9% sensitivity and 98.0%, specificity. The model had an excellent performance in terms of less processing time than existing methods.

Using U-Net model and ConvNet, Dong *et al.* (2017) developed an automated brain tumor segmentation method. They collected 54 low-level tumor (LLT) and 220 high-level tumors (HLT) cases from BRATS 2015. The approach proved effective with promising segmentation after Cross-validation. Deep convolutional networks and U-Net obtained equal outcome for the absolute tumor region as well as high quality results for tumor core region. Without requiring manual intervention, the suggested approach may be modified to patient's actual brain tumor segmentation techniques.

Sedlar *et al.* (2017) proposed and demonstrated segmentation of brain tumors using a multi-path CNNs technique to distinguish between lesions and healthy brain regions. Using BraTS dataset (2017), the average Dice score was, increased tumor: 0.6049%; total tumor: 0.8436% and core tumor: 0.6938%. Antropova *et al.* (2017) proposed a methodology for classifying benign and malignant breast tumor cells. The data set contained 690 MRI images, 245 mammography cases, and 1,125 ultrasound cases from three distinct imaging modalities. With traditional CADx and CNN features, a nonlinear (SVM) was used for classification. For performance evaluation, AURC was determined. The AURC instances for MRI were 0.89, mammography cases of 0.86, and ultrasound cases of 0.90, according to the researched findings.

Sukh *et al.* (2017) developed a model that evaluates the demonstration of deep ensemble learning On MRI brain tumor scan images. 805 patients' MRI brain images were included in the collection. They devised a framework based on a hybrid of deep structured learning and scanty regression. The CNN architecture used during the investigation has three convolutional layers which were clustered together and completely linked. MOLR regression and JLLR were used to compare the DeepSet Sparse Regression Network (DeepESRNet) to two other approaches (JLLR). DeepESRNet's and MOLR have an accuracy of 90.28% while DeepESRNet and JLLR have an accuracy of 91%, according to the studies researched.

Xue *et al.* (2018) used x-ray images to classify osteoarthritis of the hip joint. Two radiologists with over 20 years of expertise sorted the 420 images into osteoarthritis and normal views. The osteoarthritis group contained 201 images, whereas the normal group contained 219 images. VGG-16, a deep learning CNN with 16 layers, was utilized to classify the data. The performance of the neural network was compared to that of a radiologist with ten years of expertise. The neural network obtained the result of 92.8% of accuracy, 95% of sensitivity, and 90.7% of specificity, respectively.

Wang *et al.* (2017) developed a cascaded segmentation technique for glioma sub-region using a multimodal brain MR dataset. In order to segment the whole tumor, augmented tumor and tumor core, three networks approaches were used. The findings demonstrated that the proposed technique improved, and tumor core segmentation with Dice scores of 0.786% for tumor core, 0.905% for whole tumor, and 0.838% for tumor segmentation respectively.

Liu *et al.* (2018) developed deep learning model to identify brain illnesses. Cue-based deep learning approaches were used in their study as data driven in learning method. Three data sets were used: A-DNI1, A-DNI2, and MIRIADs. Deep learning based on landmarks can learn images from start to finish, extracting local and global features. According to the findings of the study, the suggested technique attained an accuracy of 92.75% with an AUC of 97.16% on the A-DNI1 dataset. The accuracy of the A-DNI2 dataset was 91.09% with an AUC of 95.86%. Their method has 92.75% for accuracy and 97.16 % for AUC respectively on the MIRIADs dataset.

Sobhaninia *et al.* (2018) developed a new approach for CNN to automatically segment the most prevalent type of tumors which include glioblastoma, meningeal, and pituitary tumors. The results show that image segmentation accuracy improved when using an angle base segmentation. The highest dice score of 0.79% was achieved, which correlated with image of the sagittal perspective. The lowest dice score of 0.71% which correlated with image of the axial view of the head was also discovered The technique used does not require pre-processing steps.

Using BRATS 2015, Seetha *et al.* (2018) developed an automated brain tumor classification model and engaged Fuzzy C-Means segmentation approach for shapes, texture and feature extraction. When compared to existing approaches, the CNN achieved 97.5% accuracy with little complexity (SVM and DNN).

Das *et al.* (2019) proposed a CNN model that can classify brain tumor in T1-weighted contrast-enhancement in MRI images and using CNN to categorize the pre-processed image. Three brain tumors were among the data obtained (glioma, meningioma, pituitary). Using the CNN model, the result obtained was 94.39% for high accuracy, 93.33% for precision and 93% for recall respectively.

Abiwinanda *et al.* (2019) used a CNN model to identify the three most prevalent types of brain cancer: pituitary, gliomas, meningiomas. Online BRATS (2017) was used for data collection information on brain tumors. At best, results achieved 98.51% for training accuracy and 84.19% for validation accuracy.

Kermi *at el.* (2019) developed complete automatic and efficient brain tumor segmentation methodologies. They used a modified U-net architecture to focus on 2D DNNs. The proposed approach used pre-operative multimodal 3D-MR imaging to extract the whole tumor and intra-tumor regions, including growing tumor, necrosis and edema. The segmentation algorithm was evaluated and tested on many patients with HLG and LLG tumors using the BRATS 2018 dataset. The results obtained good Dice score of 0.783% for enhancing tumor, 0.868% for the total tumor, and 0.805% for tumor core, respectively. To increase execution performances of segmentation in the tumor core, active tumor regions, and proposed technique may be improved upon by employing ensemble learning methods such as Stack and Blend.

Mittal *et al.* (2019) used the Undicimated wavelet transform and Growing Convolutional neural network to present a better tumor segmentation approach for MRI Brain Imaging Scan (GCNN). The developed method was compared to K-NN, SVM, SOM, GA, and CNN approaches. The results obtained were computed on 2,457 MR images Scan from the BRAINIX

dataset. In terms of computation, GCNN has the lowest value with 0.4s compared to CNN with 1.6s, GA with 3.2s, SVM with 2.7s, SOM with 4.2s, and K-NN with 3.8s. In real-time applications, the suggested method suites brain tumor segmentation.

Thaha *et al.* (2019) used the BAT method to develop Enhanced Convolutional Neural Network (ECNN). To develop deep CNN model, they focused on small Kernels. The precision, recall, and accuracy of ECNN are compared to the current CNN algorithm of Pereira *et al.* (2016) for utilizing the Brain Tumor Segmentation Challenge (BRATS 2015) dataset. Findings revealed on the one hand that the developed ECNN model achieves greater precision of 87%, recall of 90%, and accuracy of 92%. The present CNN approach, on the other hand generates 82%, 85%, and 89%of the time. To increase accuracy, they suggested using a variety of the approaches.

Wang *et al.* (2019) expanded on (Wang *et al.* 2017) they advocated the use of CNN to improve automated multi-class brain tumor segmentation in real time-testing. The fundamental network topologies were 3D U-Net, 2.5D multi-class WNet and cascaded networks. To train as well as testing the model, they used data from BRATS 2018. According to findings, test-time augmentation enhances accuracy of segmentation for a variety of CNNs, including the 3D UNet (Çiçek *et al.*, 2016), multi-class WNet, and cascaded networks (Wang *et al.*, 2017).

Menon *et al.* (2020) using CNN, he proposed an automated technique for segmenting and classifying brain tumors. They utilized patch-wise techniques to segment MRI images from the BRATS dataset. The results showed approximately 95.6% accuracy on the test dataset. To improve the spectral location of gilomas in the glilac cells, they used a combination of deep neural networks and CNN.

Rehman *et al.* (2020) presented the BU-Net 2D image segmentation approach to assist brain tumor segmentation. They employed RES (residual extended skip) and a broad context (WC). The model was tested using the BraTS2017 HGG datasets. The proposed BU-Net outperforms already available current update approaches such as (3DU-Net, S3DU-Net, U-Net, ResU-Net, Ensemble Net, TTA, and MCC). In comparison to the 3D U-Net, it indicated that the 2D U-Net demonstrates less information loss.

Overall, in this paper, some image segmentation techniques have been presented. These techniques are capable of extracting input image characteristics and classifying these characteristics. However, these image segmentation techniques' limitations stem from the challenges they are faced with the following:

a.complex and irregular morphology,

b.anatomical variability of the patient,

c.observer-to-observer variation and

d.time - consuming and error-prone during the manual analysis of brain MRI.

Therefore, CNNs have recently demonstrated exceptional image segmentation performance. It is not surprising that CNN excel in segmentation of brain tumor. It can't even come close to matching the categorization performance of current approaches. The architecture such as U-net and Mask-RCNN must be adapted. In the methodology section, CNN model will be proposed, the results obtained in the learning and testing phase will be interpreted and discussed.

Our Contribution

We aimed to implement and evaluate CNN by incorporating a U-Net and Mask-RCNN architecture to detect automatic segmentation of brain tumors. Some image segmentation techniques have been presented; these techniques are capable of extracting input image.

- The proposed deep learning models developed in this research were executed using Python programming language, managing Keras with TensorFlow as the backend.

- We investigated effectiveness of the network architectures U-net and Mask-RCNN for segmentation of brain image. A total of 253 public brain tumor datasets were used in this research. 70% of the images were in the training dataset, while testing consisted 30% of the data utilized to validate the proposed approach. For training, there were 176 images, and for testing, there were 77. Each one has a 240x240 capacity. (Background (label 0), necrotic and non-enhancing tumor (label

1), edema (label 2) and enhancing tumor (label 4) for enhancing tumor were the labels used for tumor segmentation. T1- and T2-weight modalities were present for each brain co-registered image. As shown in Figure 20 Necrosis, Edema, Non-enhancing core and enhancing core are the four tumor classes represented by each gray level, from low to high. The first column shows the two brains MRI scans with T1 modalities used, the second column, the ground truth.

- We evaluated the effectiveness of non-tumor and tumor classification, an error matrix also known as confusion matrix was obtained using abbreviated formulas such as True positive (TP), False positive (FP), True negative (TN), and False negative (FN) cancers were represented in the matrix. The training model achieved 93% for accuracy, 95% for sensitivity, and 90% for specificity. The similitude between forecasted and the ground truth is at 96%. As described in Zijdenbos *et al.* (1994), a good overlap occurs when DICE >0.700. Based on this analysis, the training model has demonstrated good results. The testing set (77 cases) results showed that the proposed model had 89% for sensitivity, 86 % for specificity and 88% for accuracy. The overall (253 cases) achieved 92% for a sensitivity, 88 % for specificity and 90.5% for an accuracy rate. The computation and running time of the trained model for segmenting the 176 datasets was approximately 7 minutes 45 seconds.

- The research effectively demonstrated the application and strength of the deep learning algorithm concepts in brain tumor diagnosis. Results from our U-net and Mask RCNN however proved that deep learning approach is reliable and improve automatic segmentation accuracy in medical image in such a way that has been presented in this research work.

In comparison to other related literature reviewed in this research, the proposed hybridized CNN models for segmentation and classification of a brain tumor using 253 MRI dataset from (Kaggle, 2019), Mask – RCNN and modified U- nets CNN models were used for extraction and segmentation of a brain tumor region of interest. These include Necrosis, Edema, Enhance region and Not-enhanced region. The dataset was divided into two parts: (a) Training and (b) Testing. The model was evaluated by using 170 datasets for training and 77 datasets for testing. The model achieved high accuracy index of 90.5% and Dice similarity coefficient of 0.96% with less execution time of 47 seconds to segment a whole 253 brain tumor dataset. The proposed model has effectively demonstrated the strength of the deep learning algorithm and Convolutional neural network models in brain tumor segmentation processes.

3. METHODS

This research was based on empirical approach and aimed to segment Intracranial Neoplasm tumor from brain MRI scan images using Mask R-CNN and U-net convolutional neural networks. Data were collected from the publicly kaggle dataset. Datasets, data pre-processing, network structural designs, training and testing processes, and proposed ensemble methodologies are all described in this section. Conceptual perspectives are offered for the proposed CNN architecture, deep learning segmentation of brain tumor MR images and how segmentation approach improves image categorization. The segmentation process begins with data preparation in the dataset. After preparing the data, next is data visualization. Following that, augmentation of data is used to assist enhancement of the training set. Mask R-CNN and U-net models' actual training using brain MRI images is done to segment tumors from the brain. The model was evaluated to determine performance base on the accuracy, sensitivity, specificity, and dice coefficient metrics.

3.1 Data Collection and Techniques

This section includes a collection of publicly available brain MRI datasets, as well as an analysis of those datasets. The overall procedures, as described in Figure 1 include four main stages, such as: data pre-processing, data preparation, image segmentation, and data post processing. After collections of the dataset, the next step is the data pre-processing using skull stripping, correction of bias field, registration of image, and extraction of brain techniques. Then the output is forwarded to Patch extraction method and data augmentation. The dataset was split into two parts during the segmentation of processed MR scan images, with 70% of the dataset being used to train the network and 30% used to test or assess the proposed model's final result.

Novelty Journals

ISSN 2394-7314

International Journal of Novel Research in Computer Science and Software Engineering
Vol. 11, Issue 2, pp: (25-44), Month: May - August 2024, Available at: www.noveltyjournals.com

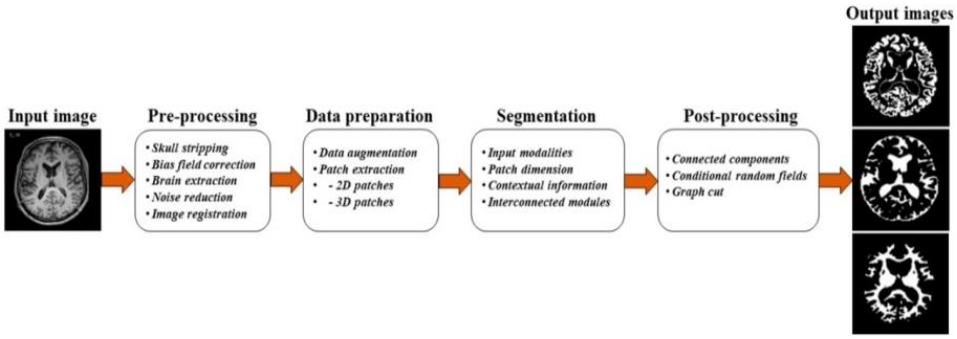

Figure 1: Flow Chart for Brain MRI Analysis (Source: Duta *et al*, 1998)

3.2 Experiment Dataset

This study used the Intracranial Neoplasm MRI scan brain tumor dataset for brain tumor segmentation sourced from kaggle.com a shared dataset platform is usually used for machine learning competitions. The dataset contained 253 records, with 155 records. The imaging datasets are all available and accessible as ZIP files (tar.gz) and describe both native (T1) and T2-weighted images. Figure 2 shows one enlarged screenshot sample of JPG MRI image scan from the dataset. Figure 3 shows a screenshot of brain tumor dataset from Kaggle.com. The following are the attribute of MRI dataset used in this research.

Sensitivity to Contrast: Contrast sensitivity refers to an imaging technology with an ability to produce resemblance of organs of the body with minor changes or contrast. The imaged dissimilarity takes form of a certain physical characteristic. In x-ray imaging, particularly CT, the main source of contrast is a difference in physical density. MRI has high sensitivity for seeing different diseases across tissues in the body. Specifically, it can image a wide range of properties (T1, T2). The most common MRI sequences are T1-weighted scan (short relaxation time and black in color) and T2-weighted scan (long relaxation time and white in color) (long relaxation time and white in color). To produce T1-weighted images, short TE and TR durations are utilized. The brightness of an image in MRI scan is determined by the T1-weighted properties, while T2-weighted images are made with longer (TE) echo times and (TR) repetition periods.

Details: The capacity to view tiny objects and structures within the body is a defining trait of all imaging modalities. Due to the blurring that occurred throughout the imaging process, Anatomical detail visibility is diminished (also known as spatial resolution). Blurring occur in all medical imaging modalities, although not to the same degree. MRI has more blurring than radiography as indicated in Fig 2 below. As a result, tiny objects detectable on traditional radiographs cannot be imaged with MRI.

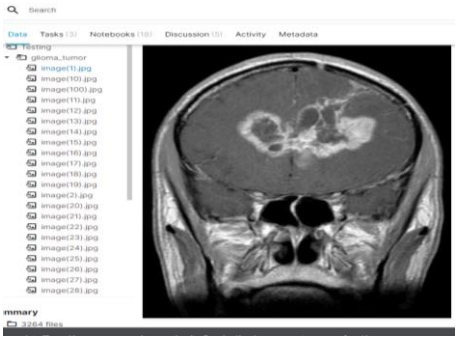

Figure 2: One sample of enlarge MRI Images

Noise: In MRI, visual noise is a significant problem. The inclusion of noise in a picture degrades its quality, particularly by obscuring low-contrast objects and tissue differences. Images with various amounts of visual noise are shown in Figure 3. The majority of the noise in MR image is caused by undesired RF radiation picked up from the patient's body.

Artefacts: Unwanted things in photographs that do not directly reflect an anatomical feature, such as streaks and dots. They are usually induced by interactions between the patient's body or biological processes (such as movement) and the imaging method.

Spatial: The size of the imaging voxels influences the overall spatial resolution of MR images. Hence, voxels are equilateral solids in three dimensions; they vary greatly in each direction. As a result of the resolution, the voxels is affected by the matrix size, field of view, including slice thickness. When establishing an imaging technique, spatial features need to be considered in the condition of overall image quality. Image detail and image noise are heavily influenced by voxel size.

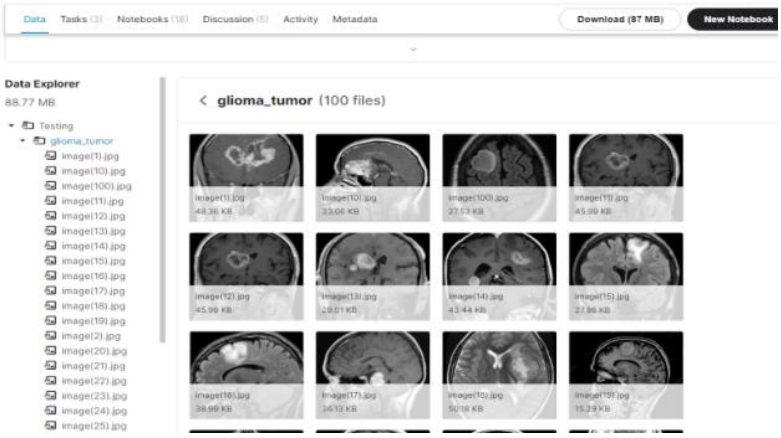

Figure 3: Screenshot of MRI Brain Tumors from Kaggle.com

3.3 Data preprocessing

After collecting an MRI, different preprocessing method are required so that the images can be used to segment prominent types of brain tissue. Figure 4 depicts preprocessing instances of brain MRI. MRI preprocessing includes extraction of brain, correction of bias field, and registration of image.

Brain extraction: Tissue and sections of the spinal cord, head, skull, fat, and eye are visible on the brain MRI. Skull pillage is required to segment brain matter and non-brain matter in order to establish whether volumes of pixels are brain matter or non-brain matter.

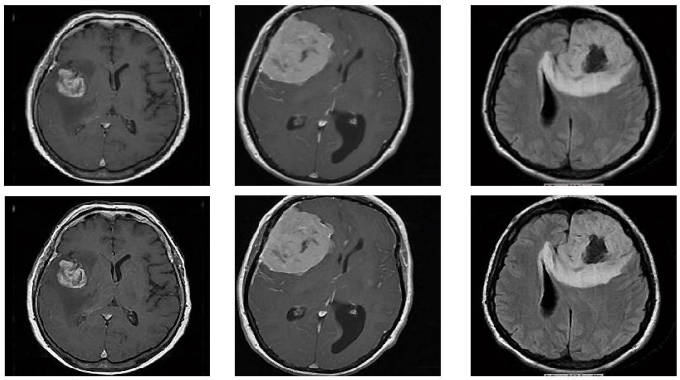

Figure 4: Pre-processed MR images of the brain with a brain tumor

Brain skull stripping provides new image with only voxels or binary values that assigned brain voxels 1 and the rest of the matter 0. Brain voxels, which contain the brain stem, gray tissue (GT), white tissue (WT), and cerebrospinal fluid, are found throughout the cerebral cortex, subcortical areas, and cerebellum (CSF). The tissues, bones, scalp, eyes, fat, dura, muscles, and skin are all non-brain voxels.

Bias field correction: this assist fine-tunes image contrast caused by electromagnetic induction inhomogeneity. Because the bias field depends on magnetic field intensity, it is virtually non-existent when the MRI is done at 0.5 T. The magnetic field is deemed strong when its intensity is 1.5 T or 3 T, and above, and it might interfere with MRI analysis.

Image registration: The method of converting spatial image alignment to shared anatomical regions. There are two types of image registration: inter-patient and intra-patient. Intra-patient registration assists in aligning MRI definite order for T1 and T2-weighted images to provide multiple-channel description for each brain region, whereas inter-patient registration

Novelty Journals

ISSN 2394-7314

International Journal of Novel Research in Computer Science and Software Engineering
Vol. 11, Issue 2, pp: (25-44), Month: May - August 2024, Available at: www.noveltyjournals.com

aids in standardizing MRI onto stereotaxic spaces. Following preprocessing of data, preparation data is carried out from the input volumes utilizing augmentation of data or patch-based processes.

3.4 Data preparation

The researchers used augmentation of data method to considerably expand the quantity of trained specimen. Therefore, final data collection might be rather tiny. Augmentation of data will be required to enhance the dimension of the training dataset. Three transformations will be applied to each axial slice, each within a parameter range, including rotation, shear mapping, and scaling as illustrated in Figure 5. Scaling can introduce valid augmented image into a training set since tumors is in sizes. Scaling is sometimes used with trimming to retain the real image size since many deep architectures demand constant images. Equation 1 depicts how this operation S can be carried out. For the x and y bearing, the scaling factors are denoted by Sx and Sy respectively.

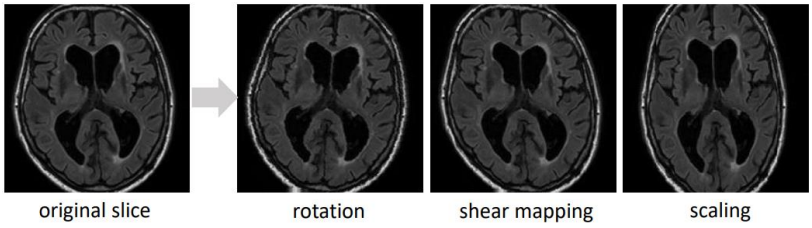

Figure 5: An Illustration of a Data Augmentation result

$$S = \begin{pmatrix} S_x & 0 \\ 0 & S_y \end{pmatrix} \quad (1)$$

Shear mapping (H) is a technique that moves each point in a picture in a certain direction. As demonstrated in Equation 3, the line that passes through origin and parallels direction determines the displacement where

$$H = \begin{pmatrix} 1 & h_x \\ h_y & 1 \end{pmatrix} \quad (2)$$

shear coefficients of x and y directions are represented by hx and hy respectively. Rotation (R) rotates an image around angle α by the center of the pixel. The rotational execution is followed by an appropriate interpolation to suite the real image size. As illustrated in Equation 3, the R rotation operation is frequently combined with 0 padding put-in to the lost pixels.

$$R = \begin{pmatrix} cos\ \alpha & -sin\ \alpha \\ sin\ \alpha & cos\alpha \end{pmatrix} \quad (3)$$

In clinical practice, the parameter range indicates variance in several features across images; for example, The brain rotates in a range of [-15, 15]. Each of the three transformations' parameter ranges are shown in Table 1. After performing the changes, Figure 5 displays an example of the resultant slices.

3.5 Post processing

Many post-processing approaches have been proposed to eliminate false positives and enhance segmentation findings. Manual adjustment thresholds are used in traditional post processing techniques like thresholding or regional growth-based approaches to emphasize isolated regions or pixels. (CRF) and (MRF) are recently utilized to deduce pixel pairings from previously collected data such pixel strength distributions and space-based distance.

TABLE 1: Data Augmentation Parameters Ranged

Methods	Rotation	Scaling	Shearing	
Parameters	[-15◦, 15◦]	[0.9, 1.1]	[-0.1, 0.1]	[-

Novelty Journals

ISSN 2394-7314

International Journal of Novel Research in Computer Science and Software Engineering
Vol. 11, Issue 2, pp: (25-44), Month: May - August 2024, Available at: www.noveltyjournals.com

At the post-processing step, the CRF was employed with the energy function for image segmentation tasks. Equation 5 shows how to formulate it.

$$E(x) = \sum_i \theta_i(x_i) + \sum_{ij} \theta_{ij}(x_i, x_j) \quad (4)$$

Where x is the label assignment for pixels. $\theta_i(x_i)$ is called unary potential and $\theta_{ij}(x_i, x_j)$ called pairwise potential. Those Equations are described as following.

$$\theta_i(x_i) = -log\ P(x_i) \quad (5)$$

Where $P(x_i)$ is the label assignment probability at pixel I as computed by the ensembling model (U-net and Mask R-CNN),

$$\theta_{ij}(x_i, x_j) = \mu(x_i, x_j)\left[\omega_1 exp\left(-\frac{\|p_i - p_j\|^2}{2\sigma_\alpha^2} - \frac{\|I_i - I_j\|^2}{2\sigma_\beta^2}\right) + \omega_2 exp\left(-\frac{\|p_i - p_j\|^2}{2\sigma_\gamma^2}\right)\right] \quad (6)$$

where $\mu(x_i, x_j) = 1\ if\ x_i \neq x_j$.

The first phrase in parentheses checked pixel values and pixel locations to ensure that pixels in close proximity have the same categories. The second, is used to keep away tiny areas remote from other regions that have been indicated as positive - tumor regions in this case.

Data augmentations are carried out to increase training data using scaling, shear mapping and rotating. U-nets and Mask R-CNN segmentation schemes were applied into the prepared dataset to segment the proposed regions of interest (ROI). The following criterion was used to evaluate the model: sensitivity, specificity, accuracy, Jaccard index, DICE. Lastly, the model predicts the output based on knowledge discovery and decides whether the patient is diagnosed for brain tumor or not. Figure 6 shows the flow of proposed segmentation models. The first U-net convolutional layer used the augmented data for the data layer. During the encoder and decoder processes, each identified object in the original image is

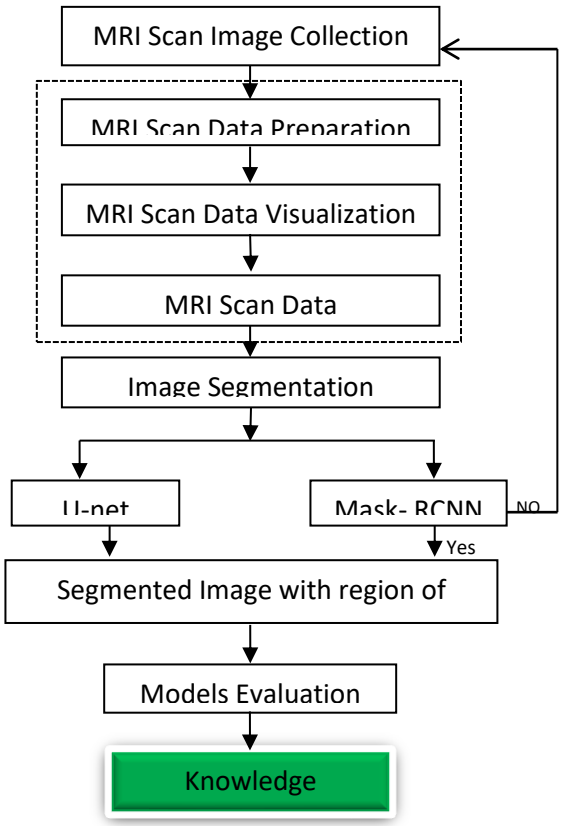

Figure 6: Flow of the Proposed Segmentation Model

Novelty Journals

ISSN 2394-7314

International Journal of Novel Research in Computer Science and Software Engineering
Vol. 11, Issue 2, pp: (25-44), Month: May - August 2024, Available at: www.noveltyjournals.com

compared to the same detected object in the augmented images. The procedure is continued until the majority voting condition is met in theory. After that, the U-net final convolutional layer generated pixel-wise classification scores that are normalized using the softmax function. Shown in Equation 7. during the training phase.

$$p_k(x) = \frac{exp(a_k(x))}{\sum_{k\prime=1}^{k} exp(a_{k\prime}(x))} \quad (7)$$

Therefore, ak(x) is the initial attribute in channel k at the pixel location x, while k is the number of classes.

3.6 The Proposed Model's Conceptual View

The research uses the U-net and Mask-RCNN architecture to develop a hybridized deep learning method. Figure **7** depicts the proposed methods conceptual view. During both training and testing, a redesigned form of U-nets approach presented by Isensee et al. (2017) was utilized, where two modalities of axial slices brain MRI were accepted as input, Figure **8** depicts the U-net architectural network. To enhance brain tumor segmentation performance, U-nets model was utilized, which included: (i) the feature representation of the input image was obtained using encoder or down-sampling convolution network and (ii) A decoder or convolutional network was utilized to generate segmentation from a feature representation of the input image. Mask - RCNN is the second architecture applied for the segmentation of brain tumor in this research. It has the following phases: (a) to propose possible bounding boxes, the region proposal network (RPN) is utilized and (b) Network head layers. Based on the above analysis, the model proposed a separated training approach in the first time and merging of the two architectures such as U-nets and Mask-R CNN at the end. The proposed segmentation approaches for brain tumor image segmentation include four procedures: one is pre - processing and augmentation data set; trained model and merged model; and finally segmentation result is obtained.

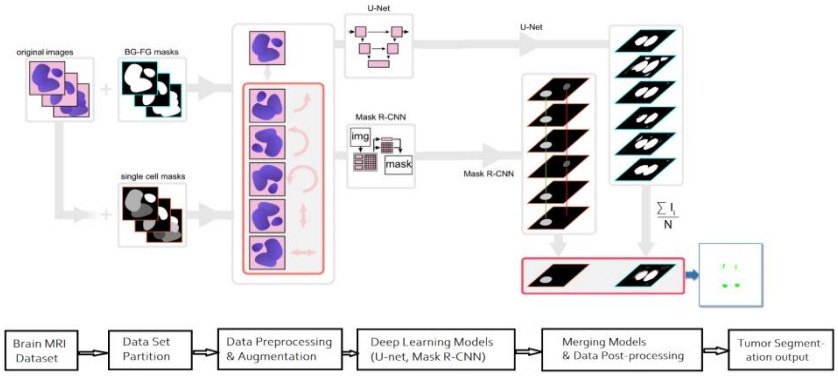

Figure 7: Proposed Segmentation Conceptual View Model

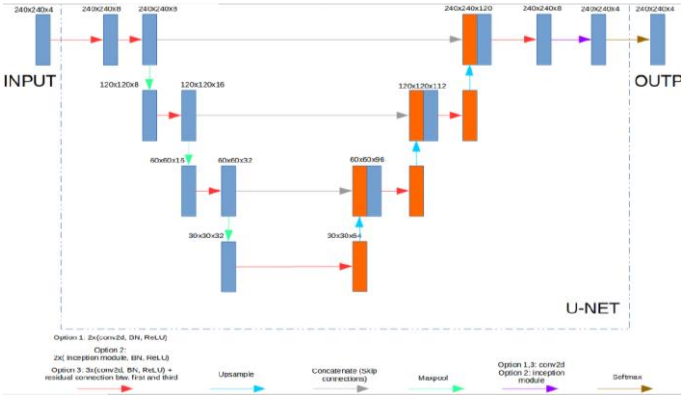

Figure 8: The U-nets Architecture for Brain Tumor Segmentation

During the first stage, the proposed segmentation technique includes the following phases: data preparation to remove empty space from MRI scan images and to resize and crop images to get the desired image dimensions; data visualization to better understand the structure of data. At the same time, the Mask-R CNN allocates an "individual object" each pixel with a label

in the original brain MRI. The following RPN layers, as well as the RoI Align layer, share the feature map. Regional proposals are generated via the RPN network. This layer use softmax to identify whether the anchors are positive or negative, and then employ bounding box regression to alter the anchors in order to provide accurate propositions. After synthesizing the information, The RoIAlign layer collects the input attribute map and argument, extract the argument attribute map, and sends them to the multibranch prediction network. FC layers construct a proposition category using proposition feature maps, and then utilize bounding box regression to acquire the final accurate position of the detection box and FCNN segmented instance for masking. Figure **9** is an illustration of the Mask-RCNN technique. Finally, U-net and Mask RCNN segmentation schemes are merging and segmented ROI is obtained. At this stage, the model uses a deep learning algorithm to anticipate the output based on past information and determine if the patient has a brain tumor or not. The models' evaluation is done to ascertain performance based on the following metrics (accuracy, precision, and recall, dice coefficient, Jaccard similarity index). Accuracy is defined as the ability to accurately discern between healthy and unhealthy situations. The term "specificity" refers to the ability to correctly identify healthy situations. Sensitivity is defined as the capacity to appropriately identify malignancies. A statistical tool for comparing segmentation and ground truth is the dice similarity coefficient. The Jaccard similarity index determines how closely two sets are related.

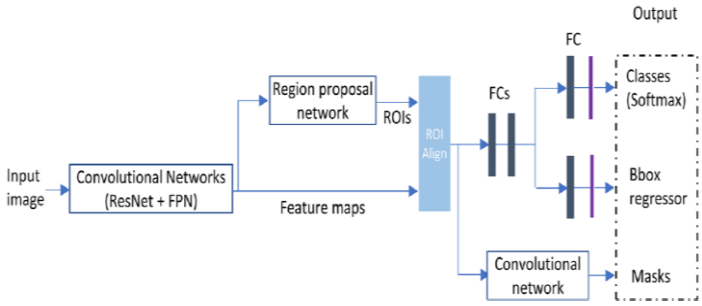

Figure 9: Architecture of the Mask R-Convolutional Neural Networks

3.7 Proposed Algorithm for Brain Tumor Segmentation

The segmentation of brain tumor approach makes use of deep neural network model to segment and extract brain tumor regions. The proposed algorithm takes input as 4 sub-types of the brain tumor annotated MRI and outputs the mage. The algorithm used for segmentation explains how U-Nets and Mask -RCNN works.

Deep Learning Algorithm of Brain Tumor Images Segmentation

Input: Kaggle Brain Scan MRI data sets

Output: Brain Tumor Segmentation

BEGIN

1. loadImage()
2. dataPreprocessing()
3. dataAugmentation()
4. splitdata()
5. loadUNETModel()
6. **for** each epoch to epochNumber **do**
7. **for** each batch to batchSize **do**
8. Auto-encoder regularization
9. Concatenation
10. Apply softmax()

11. Segmented image of Unet

12. **endfor**

13. **endfor**

14. X ← Segmented image of Unet

15. load MaskRCNNModel()

16. Fine-tune the RPN

17. rain a Fast R-CNN object detection model

18. initialize RPN training

19. repeat 17,18 to train RPN and Fast R-CNN alternatively if needed

20. Y ← Mask Predicted

21. Merge MaskRCNNModel() + UNETModel()

22. X ← X+Y

23. Apply csf()

24. **if** csf() >= 1

25. Output ‘’ diagnosed for brain tumor’’

26. **else**

27. Output ‘’ not diagnosed for brain tumor’’

28. **end if**

END

4. EVALUATION METRICS FOR BRAIN MRI SEGMENTATION

This section explains the metrics used to evaluate segmentation. These metrics include, performance precision, specificity, sensitivity, and the dice coefficient, as well as the Jaccard index.

Accuracy, Sensitivity and Specificity.

True Positive(TP) and False Negative (FN) were used to evaluate the accuracy, sensitivity and specificity of the proposed technique. Equation 8 can be used to calculate accuracy, which is defined as the ability to properly discern between healthy and unhealthy situations. The term "specificity" refers to the ability to correctly identify healthy situations. Equation 9 is used to calculate it. Sensitivity is defined as the capacity to appropriately identify malignancies. Equation 10 is used to calculate it.

$$Accuracy = \frac{TN + TP}{TN + FP + TP + FN} \quad (8)$$

$$Specificity = \frac{TN}{TN + FP} \quad (9)$$

$$Sensitivity = \frac{TP}{TP + FN} \quad (10)$$

Similarities dice coefficients

The dice similarities coefficients are statistics used in comparing the similarity of segmentation and ground truth. The positive result aspects that are equivalent to the ground truth are discovered first, thereafter, the total number of positives in both is divided by the result. Let A and B be the binary segmentation labels for one tissue class on pixels created manually and computationally, respectively, for a certain patient. Equation (11) is used to obtain the dice ratio.

$$DICE = \frac{2*|A \cap B|}{|A|+|B|} = \frac{2*(TP)}{2*(TP)+(FN+FP)} \quad (11)$$

Where by |A| indicate the positive number of components in the binary segmentation, and |AB| indicate the number of elements that are positive shared by A and B. The Dice ratio lies between [0, 1], and the largest value represent a higher accuracy of the segmentation.

Jaccard index

The Jaccard similarity index determines how closely two sets are related. It is represented in Equation (12). It's calculated by dividing the sets' intersection by their union.

$$J = \frac{|A \cap B|}{|A \cup B|} = \frac{\text{TP}}{\text{TP} + \text{FP} + \text{FN}} \quad (12)$$

Additional metric to evaluate the rapidity of segmentation the computation time of automatic segmentation was calculated. The following processing time were considered: loading image time (T_i); time to extract the binarized image (T_b); time to load the U-net model (T_{unet}); time to load the Mask R-CNN model ($T_{maskrcnn}$); time to load the evaluation metric (T_{ev}). The total processing time considering all the times generated in the segmentation, will be

$$T_{ps} = T_i + T_b + T_{unet} + T_{maskrcnn} + T_{ev} \quad (13)$$

5. RESULTS

This section presents the result of the suggested model which is segmentation details. Augmentation of data, preprocessing are utilized in training the deep learning model. The network architecture's efficiency was measured through series of tests for brain image segmentation that employed U-net and Mask-CNN. The segmentation results obtained are presented, assessed based on dataset using evaluation metrics on HP system with 12GB RAM; the proposed architectures are trained and tested.

5.1 Simulation Experiment

This section shows the proposed model findings based on the dataset from Kaggle.com. The dataset from Kaggle.com were used both to test and to train the model. The obtained results of this research are based on convolution layers U-net and Mask-CNN. The public kaggle.com dataset was utilized as the experimental dataset and randomly divided into training as well as testing. In the whole datasets, the training set comprises 70% images. The testing set also comprises 30% of the data and is used to validate the proposed approach. DICE, accuracy, sensitivity, and specificity were all employed in the experiment as assessment indices.

5.2 Experiment environment

The deep learning model presented in this work was built in Python programming language using Keras together with Tensor Flow as backend. All of the tests were carried out on a personal computer that ran Windows 64 bit, executing on 2.40GHz; Intel Core7 CPU; 12GB RAM; and 2 GB GDDR5 memories NVidia Quadra K2000 GPU.

5.3 Experiments on Kaggle dataset

The dataset was partitioned in two sections: the training as well as testing. To evaluate the model accuracy, out of 253 image datasets, 176 were utilized for training and 77 for testing with distinct image types (jpeg and jpg). Each of the images has a 240x240 square inch capacity. Tumor segmentation was carried out using four labels: background (label 0), necrotic (label 1), non-enhancing tumor (label 2), edema (label 3), and enhancing tumor (label 4). Each brain co-registered image had T1- and T2-weight modalities. Table 2 explains the segmentation datasets used in the experiments. Figure **10** provides an example of the brain tumor detection image and the ground truth.

TABLE 2: The Image Segmentation Experiments Dataset

Dataset	Image	Input size	Modality	Provider	Type
Training	176	240x240	MRI	Kaggle.com	Jpeg, jpg
Testing	77	240x240	MRI	Kaggle.com	Jpeg, jpg

Novelty Journals

ISSN 2394-7314

International Journal of Novel Research in Computer Science and Software Engineering
Vol. 11, Issue 2, pp: (25-44), Month: May - August 2024, Available at: www.noveltyjournals.com

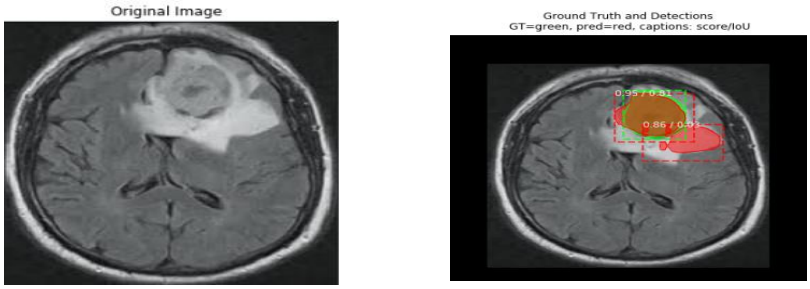

Figure 10: MR Image Used as Input and a Sample of Ground- Truth for Edema, Tumor, and Non-Tumor

5.4 Experiments on segmentation dataset

The training data was used to build the segmentation model, while testing data was used to measure the efficiency. The computer system was used to store the MR image. After importing the python libraries used throughout the simulation (matplotlib, numpy, pandas), the list directory is saved in a variable. The mask image is pre-processed by scaling it and normalizing the pixel value, which was subsequently stored at the same index position in the output array as the pre-processed mask image. The image is stored in X[n], while the mask is stored in Y[n]. At each step of the pre-processing step, a plot of the pre-processed image is done to get the sub-results. Figure 11 shows both the pre-processed image and its mask. The next phase is to segment the pre-processed images and load all the relevant functions into the libraries from that segmentation method. The dataset was divided into two sections: X is for training while Y is for testing of the model. After splitting, the weights were loaded and the convolution libraries used (U-net and Mask-R) was imported as a backbone network. Both results (U-net and mask-R) were thereafter merged. The final output wass then reshaped to 28x28. The model has assembled and fitted the training and validation data to the model after defining everything. After training the model, it evaluates its performance over the testing set. The trained model saved weights by serializing them after assessment. After the model is saved, predictions are made and saved using the trained model on X train and X test (see Figure 11).

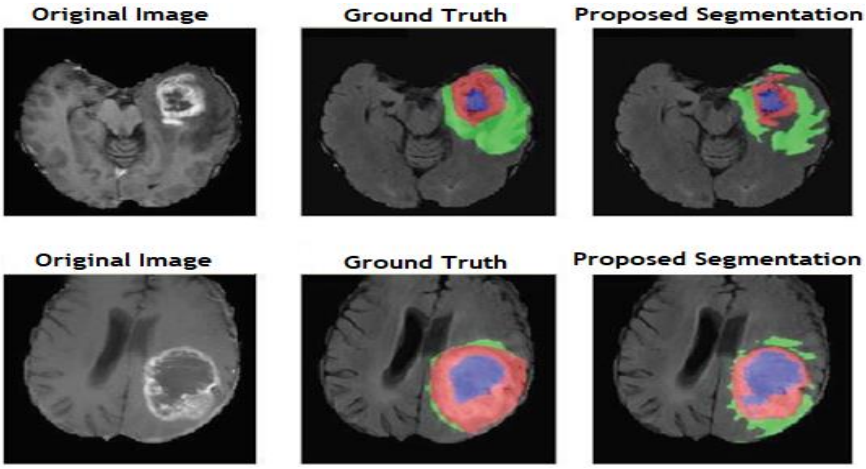

Figure 11: The Proposed Model's Segmentation Results

The brain tumor images, masks related ground truth, and the proposed models projected mask are shown below. From low to high, each gray level indicates one of four tumor classifications: (i) necrosis, (ii) edema, (iii) non-enhancing core, and (iv) enhance core. The first column shows the two brains MRI scans with T1 modalities used, the second column, the ground truth. The proposed designs' segmentation results obtained are displayed in the last column. Necrosis (NCR), edema (ED), non-enhancing (NE), and enhancing (ET) tumors are represented by the red, green, blue, and yellow, sequentially.

5.5 Points of Methods

To evaluate non-tumor and tumor classification performance, an error matrix also known as confusion matrix was formulated using True positive (Tp), True negative (Tn), False positive (Fp), and False negative (Fn) tumor was all represented in this matrix. The confusion matrix got from the training data is shown in Figures 12 and 13, while the test data is based on experimental results. TP and TN classify correctly, with TP indicating aberrant brain scan image as (True

positive) and TN indicating normal brain scan image as (True negative). Both FP as well as FN incorrectly classifies tumors, with FP displaying normal brain images as positive tumors and FN displaying aberrant brain images as negative tumors. As Figure 12: shows, while 95 of the 176-training brain tumors dataset were identified, “yes”, tumors (TP) and the 5 tumors dataset were incorrectly labeled as "no" tumors (FN). Only 7 tumors were misclassified as "no" (FP) while 69 tumor were detected as "yes" (TN). Concerning the confusion matrix obtained from test data on top of Figure 13: 42 of the 77-testing brain tumors dataset were identified as “yes” tumors and 5 for “no” tumors. At the bottom of Figure 13, 26 identified as “yes” tumors while 4 classified as “no” tumors. Sensitivity, specificity, accuracy, Jaccard index, and DICE were used to evaluate the model.

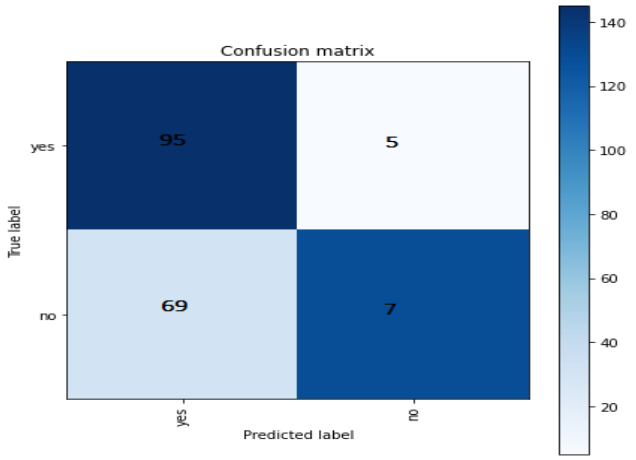

Figure 12: Obtained Confusion Matrix for Training Data in Classification

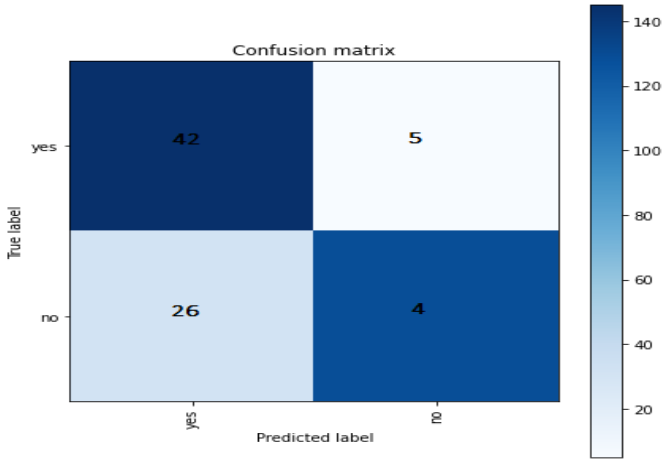

Figure 13: Obtained Confusion Matrix for Testing Data in Classification

Table 3 and Table 4 illustrate performance measure indices and results for the training and testing model, respectively. According to Table 3, the training model successfully diagnoses 93 cases out of 100. The training model was able to reach 93% for accuracy, 95% for sensitivity and 90% for specificity. The similarity between predicted as well as ground truth is at 96%. As described in Zijdenbos *et al.* (1994), a good overlap occurs when DICE >0.700. Based on this analysis, the training model has demonstrated good results. The testing set (77 cases) results indicated that the proposed model had a 89% for sensitivity, 86% for specificity and 88% for accuracy as indicated in Table 4. The overall (253 cases) achieved 92% for sensitivity, 88 % for specificity and 90.5% for accuracy rate as shown in Table 5. The computational time T_{ps} of the proposed deep learning algorithm per test image was calculated by adding loading image time (T_i); segmentation time (T_b); U-net model loading time (T_{unet}); Mask R-CNN model loading time ($T_{maskrcnn}$); and evaluation metric time (T_{ev}). The running time of the trained model for segmenting the 176 datasets was approximately 466 seconds approximately 7 minutes 45 seconds as shown in Table 6.

Novelty Journals

ISSN 2394-7314

International Journal of Novel Research in Computer Science and Software Engineering
Vol. 11, Issue 2, pp: (25-44), Month: May - August 2024, Available at: www.noveltyjournals.com

TABLE 3: Results of Evaluation Performance for Training the Model

Metrics	Equations	Process	Results
Accuracy	$\frac{TN + TP}{TP + FP + TN + FN}$	$\frac{95 + 69}{95 + 7 + 69 + 5}$	0.93
Sensitivity	$\frac{TP}{TP + FN}$	$\frac{95}{95 + 5}$	0.95
Specificity	$\frac{TN}{TN + FP}$	$\frac{69}{69 + 7}$	0.90
Dice	$\frac{2(TP)}{2(TP)+(FN+FP)}$	$\frac{2*95}{2*95+5+7}$	0.96
Jaccard Index	$\frac{TP}{TP + FP + FN}$	$\frac{95}{95 + 7 + 5}$	0.88

TABLE 4: Results of Evaluation Performance for Testing the Model

Metrics	Equations	Process	Results
Accuracy	$\frac{TN + TP}{TP + FP + TN + FN}$	$\frac{42 + 26}{42 + 4 + 26 + 5}$	0.88
Sensitivity	$\frac{TP}{TP + FN}$	$\frac{42}{42 + 5}$	0.89
Specificity	$\frac{TN}{TN + FP}$	$\frac{26}{26+4}$	0.86
Dice	$\frac{2(TP)}{2(TP)+(FN+FP)}$	$\frac{2*42}{2*42+5+4}$	0.90
Jaccard Index	$\frac{TP}{TP + FP + FN}$	$\frac{42}{42 + 4 + 5}$	0.82

TABLE 5: Evaluation of Performance Measurement Criteria of the Whole Tumor

	Accuracy	Sensitivity	Specificity
Proposed model	90.5%	92%	88%

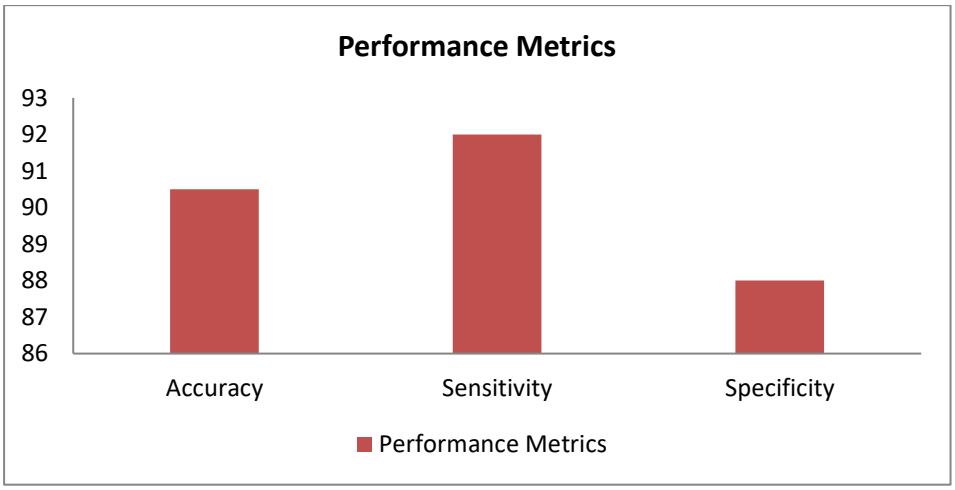

Figure 14: Evaluation of Performance Metrics

TABLE 6: Computational Time Results

Computational Time per process	T_i	T_b	T_{unet}	$T_{maskrenn}$	T_{ev}	T_{ps}
Whole dataset (Sec)	**71**	**105**	**133**	**120**	**37**	**466**

6. CONCLUSION

The segmentation of medical images remains a very broad field of research in machine learning especially the deep learning techniques that can automatically, identify and segment tumors with highest level of accuracy. In the context of cerebral imaging, the purposes of segmentation of tumor MRI images are indeed multiple: diagnostic aid, observing the patient's condition as it is progressing, and clinical test. The goal of this research is devoted to semantic segmentation of tumor (gliomas) which is among the most common brain tumors, from MRI using CNNs, which have shown its performance in recent years. The proposed technique solves issues such as computing time delays, complex and irregular morphological issues, observer to observer's variation challenge and the inconsistency of ground truth segmentations of various anatomical structures. Our solution used a modified U-net CNN. The developed deep learning models was simulated using the python programming language associated with libraries (Tensorflow, Keras), CPU 2.40 GHz, core i7 processor, 12 Gb RAM. A total of 253 public brain tumor datasets were used in this research. 70% of the images were in the training dataset, while testing consisted 30% of the data utilized to validate the proposed approach. For training, there were about 176 images, and the for testing, there were about 77 images. The results found are satisfactory, which are indicated as 90.5%, 92%, and 88% for accuracy, specificity, and sensitivity, respectively. The computation and running time of the trained model for segmenting the 176 datasets was approximately 7 minutes 45 seconds. The research effectively demonstrated the application and strength of the deep learning algorithm concepts in brain tumor diagnosis. Results from our U-net and Mask RCNN however proved that deep learning approach is reliable and improve automatic segmentation accuracy in medical image in such a way that has been presented in this research work.

REFERENCES

[1] W. Ayadi, W. Elhamzi, I. Charfi, & M. Atri, "Deep CNN for Brain Tumor Classification". *Neural Processing Letters*, *53*(1), 671–700. (2021). https://doi.org/10.1007/s11063-020-10398-2

[2] M.M. Badža, & M.C. Barjaktarović, "Classification of Brain Tumors from MRI Images Using a Convolutional Neural Network." *Applied Sciences*, *10*(6), 2020. https://doi.org/10.3390/app10061999

[3] K. R. Bhatele, & S.S. Bhadauria, "Brain structural disorders detection and classification approaches:" a review. *Artificial Intelligence Review*, *53*(5), 3349–3401. 2020. https://doi.org/10.1007/s10462-019-09766-9

[4] N. Sharma and L. M. Aggarwal "Automated medical image segmentation techniques" *Journal of Medical Physics/Association of Medical Physicists of India*, *35*(1): pp. 3-5, 2010.

[5] Y. LeCun, P. Haffner, L. Bottou, and Y. Bengio, "Object recognition with gradient-based learning" In *Shape, Contour and Grouping in Computer Vision*, pp. 319-345, 1999. Springer, Berlin, Heidelberg.

[6] Y. Chen, H. Jiang, C. Li, X. Jia, and P. Ghamisi, "Deep feature extraction and classification of hyperspectral images based on convolutional neural networks" *IEEE Transactions on Geoscience and Remote Sensing*, *54*(10): pp. 6232-6251, 2016.

[7] K. He, X. Zhang, S. Ren and J. Sun, "Deep residual learning for image recognition" In *Proceedings of the IEEE Conference on Computer Vision and Pattern Recognition*, pp. 770-778, 2016.

[8] A. Krizhevsky, I. Sutskever and G. E. Hinton, "Imagenet classification with deep convolutional neural networks" Advances *in Neural Information Processing Systems*, *25*: pp, 1097-110, 2012.

[9] P. Sermanet, D. Eigen, X. Zhang, M. Mathieu, R. Fergus and Y. LeCun, Overfeat: "Integrated recognition, localization and detection using convolutional networks" 2013. PsyA*rXiv.http//psyarXiv.com/kzy7u/preprintarXiv:1312. 6229.*.

[10] J. Long, E. Shelhamer and T. Darrell, "Fully convolutional networks for semantic segmentation" In *Proceedings of the IEEE conference on computer vision and pattern recognition*, pp. 3431-3440, 2015.

[11] Y. Chen, H. Jiang, C. Li, X. Jia and P. Ghamisi, "Deep feature extraction and classification of hyperspectral images based on convolutional neural networks" *IEEE Transactions on Geoscience and Remote Sensing*, *54*(10): pp. 6232-6251, 2016.

[12] P. Mlynarski, H. Delingette, A. Criminisi and N. Ayache, "3D convolutional neural networks for tumor segmentation using long-range 2D context" *Computerized Medical Imaging and Graphics*, *73*: pp. 60-72, 2019.

[13] D. J. Withey and Z. J. Koles, "Medical image segmentation: Methods and software" In *2007 Joint Meeting of the 6th International Symposium on Noninvasive Functional Source Imaging of the Brain and Heart and the International Conference on Functional Biomedical Imaging*, pp. 140-143, 2007.

[14] F. Milletari, N. Navab and S. A. Ahmadi, "V-net: Fully convolutional neural networks for volumetric medical image segmentation" In *2016 fourth international conference on 3D vision (3DV)*, pp. 565-571, 2016.

[15] M. Nazir, S. Shakil & K. Khurshid " Role of deep learning in brain tumor detection and classification (2015 to 2020): A review". *Computerized Medical Imaging and Graphics*, *91*, 101940, (2021). https://doi.org/10.1016/j.compmedimag.2021.101940

[16] M. Soltaninejad, G. Yang, T. Lambrou, N. Allinson, T. L. Jones, T. R. Barrick, F. A. Howe, & X. Ye, Automated brain tumour detection and segmentation using superpixel-based extremely randomized trees in FLAIR MRI. *International Journal of Computer Assisted Radiology and Surgery*, *12*(2) pp. 183–203, (2017). https://doi.org/10.1007/s11548-016-1483-3

[17] K. He, G. Gkioxari, P. Dollár and R. Girshick, "Mask r-cnn" In *Proceedings of the IEEE International Conference on Computer Vision*, pp. 2961-2969, 2017.

[18] A. Işın, C. Direkoğlu and M. Şah, "Review of MRI-based brain tumor image segmentation using deep learning methods" *Procedia Computer Science*, *102*: pp. 317-324, 2016.

[19] H. Noh, S. Hong and B. Han, "Learning deconvolution network for semantic segmentation" In *Proceedings of the IEEE International Conference on Computer Vision*, pp. 1520-1528, 2015.

[20] C. Cernazanu-Glavan and S. Holban, "Segmentation of bone structure in X-rayimages using convolutional neural network" *Advance Electrical Computing Engineering*, *13*(1): pp. 87-94, 2013.

[21] S. K. Bandhyopadhyay, and T. U. Paul "Automatic segmentation of brain tumour from multiple images of brain MRI" *International Journal Application Innovation Engineering Management 2*(1): pp. 240-248, 2013.

[22] E. Abdel-Maksoud, M. Elmogy and R. Al-Awadi "Brain tumor segmentation based on a hybrid clustering technique" *Egyptian Informatics Journal*, *16*(1): pp. 71-81, 2015.

[23] N. Nabizadeh, and M. Kubat "Brain tumors detection and segmentation in MR images" Gabor wavelet vs. statistical features. *Computers & Electrical Engineering*, *45*: pp. 286-301, 2015.

[24] X. Zhao, Y. Wu, G. Song, Z. Li, Y.Fan and Y. Zhang "Brain tumor segmentation using a fully convolutional neural network with conditional random fields" In *International Workshop on Brainlesion: Glioma, Multiple Sclerosis, Stroke and Traumatic Brain Injuries* pp. 75-87, 2016.

[25] S. Pereira, A. Pinto, V. Alves and C. A. Silva, "Brain tumor segmentation using convolutional neural networks in MRI images" IEEE *Transactions on Medical Imaging*, *35*(5): pp. 1240-1251, 2016.

[26] L. Liu, G. Zheng, J. D. Bastian, M. J. B. Keel, L. P. Nolte, K. A. Siebenrock and T. M. Ecker "Periacetabular osteotomy through the pararectus approach" technical feasibility and control of fragment mobility by a validated surgical navigation system in a cadaver experiment. *International Orthopaedics*, *40*(7): pp. 1389-1396, 2018.

[27] J. Amin, M. Sharif, N. Gul, M. Yasmin, and S.A. Shad, "Brain tumor classification based on DWT fusion of MRI sequences using convolutional neural network" *Pattern Recognition Letters*, *129*: pp. 115-122, 2017.

[28] H. Dong, G. Yang, F. Liu, Y. Mo, and Y. Guo, "Automatic brain tumor detection and segmentation using u-net based fully convolutional networks" In *annual conference on medical image understanding and analysis*, pp. 506-517, 2017.

[29] S. Sedlar, "Brain tumor segmentation using a multi-path CNN based method" In *International MICCAI Brainlesion Workshop*, pp. 403-422, 2017.

[30] D. Shen, G. Wu, and H.I. Suk, "Deep learning in medical image analysis" *Annual Review of Biomedical Engineering*, *19*, pp. 221-248, 2017.

[31] Y. Xue, T. Xu, H. Zhang, L.R. Long, and X. Huang,.Segan: "Adversarial network with multi-scale l 1 loss for medical image segmentation" *Neuroinformatics*, *16*(3): pp. 383-392, 2018.

[32] G. Wang, W. Li, S. Ourselin, and T. Vercauteren, "Automatic brain tumor segmentation using cascaded anisotropic convolutional neural networks" In *International MICCAI brainlesion workshop*, pp. 178-190, 2017.

[33] M. Bakator, and D. Radosav, "Deep learning and medical diagnosis: A review of literature" *Multimodal Technologies and Interaction*, *2*(3): pp. 47-67, 2018

[34] Z. Sobhaninia, S. Rezaei, A. Noroozi, M. Ahmadi, H. Zarrabi, N. Karimi, and S. Samavi, "Brain tumor segmentation using deep learning by type specific sorting of images: 2018. PsyA*rXiv.http//psyarXiv.com/kzy7u/preprintar Xiv:1809.07786*.

[35] J. Seetha, and S.S. Raja, "Brain tumor classification using convolutional neural networks" *Biomedical & Pharmacology Journal*, *11*(3): pp. 1457-1465, 2018.

[36] S. Das, O.R.R. Aranya, and N.N. Labiba, "Brain tumor classification using convolutional neural network" In *2019 1st International Conference on Advances in Science, Engineering and Robotics Technology (ICASERT)* pp. 1-5, 2019.

[37] N. Abiwinanda, M. Hanif, S.T. Hesaputra, A. Handayani, and T.R. Mengko, "Brain tumor classification using convolutional neural network" In *World Congress on Medical Physics and Bio-medical Engineering*, pp. 183-189, 2019.

[38] A. Kermi, I. Mahmoudi, and M.T. Khadir, "Deep convolutional neural networks using U-Net for automatic brain tumor segmentation in multimodal MRI volumes" In *International MICCAI Brainlesion Workshop*, pp. 37-48, 2018.

[39] M. Mittal, L.M. Goyal, S. Kaur, I. Kaur, A. Verma, and D. J. Hemanth, "Deep learning based enhanced tumor segmentation approach for MR brain images" *Applied Soft Computing*, *78*: pp. 346-354, 2019.

[40] M.M. Thaha, K.P.M. Kumar, B.S. Murugan, S. Dhanasekeran, P. Vijayakarthick, and A.S. Selvi, "Brain tumor segmentation using convolutional neural networks in MRI images" *Journal of medical systems*, *43*(9): pp. 1-10, 2019.

[41] G. Wang, W. Li, M. Aertsen, J. Deprest, S. Ourselin, and T. Vercauteren, "Aleatoric uncertainty estimation with test-time augmentation for medical image segmentation with convolutional neural networks" *Neurocomputing*, pp. *338*: 34-45, 2019.

[42] M.U. Rehman, S. Cho, J.H. Kim, and K.T. Chong, "BU-Net: Brain Tumor Segmentation Using Modified U-Net Architecture" *Electronics*, *9*(12): pp. 2203-2208, 2020.

[43] O. Çiçek, A. Abdulkadir, S.S. Lienkamp, T. Brox, and O. Ronneberger, "3D U-Net: learning dense volumetric segmentation from sparse annotation" In *International Conference on Medical Image Computing and Computer-assisted Intervention*, pp. 424-432, 2016.

[44] A.P. Zijdenbos, B.M. Dawant, R.A. Margolin, A.C. Palmer, "Morphometric analysis of white matter lesions in MR images:" method and validation. IEEE Trans Med Imaging 13(4):716–724, 1994.

[45] N. Duta and M. Sonka, "Segmentation and Interpretation of MR Brain Images: An Improved Active Shape Model", *IEEE Trans. Medical Imaging*, pp. 1049-1062, 1998.